Applied Petrochemical Research (2018) 8:119–129
https://doi.org/10.1007/s13203-018-0200-2

RESEARCH NOTE

Catalytic cracking of naphtha: The effect of Fe and Cr impregnated ZSM-5 on olefin selectivity

Ebrahim Mohiuddin[1] · Masikana M. Mdleleni[1] · David Key[1]

Received: 5 December 2017 / Accepted: 25 April 2018 / Published online: 4 May 2018

Abstract
This study focuses on the modification of ZSM-5 in order to enhance the catalytic cracking of refinery naphtha to produce light olefins. ZSM-5 was metal modified using different loadings (0.5–5 wt%) of Fe and Cr via the impregnation method. The metal modified ZSM-5 samples are compared and the effect of metal loading on the physicochemical properties and catalytic performance is investigated. Fe and Cr modification had an effect on both the physicochemical properties of the catalysts as well as catalytic activity and selectivity. Metal loading caused a decrease in the specific surface area which decreased further with increased metal loading. Fe had a greater effect on the total acidity in particular strong acid sites when compared to Cr. The optimum Fe loading was established which promoted selectivity to olefins, in particular propylene. Fe also had a dominant effect on the P/E ratio of which a remarkable ratio of five was achieved as well as enhanced the stability of the catalyst. Cr was found to be a good promoter for selectivity to BTX products with a two-fold increase observed when compared to Fe-modified catalysts.

Keywords ZSM-5 · Metal-modified · Catalytic cracking · Naphtha · Olefins

Introduction

Production of light olefins such as ethylene and propylene vital to many petrochemical processes has been achieved through steam cracking of hydrocarbons for almost half a century [1]. However, it is a high energy consuming process that requires temperatures in excess of 800 °C. Together with other disadvantages such as high CO_2 emissions, limited control over the propylene/ethylene (P/E) ratio and increasing propylene demand, has led researchers to identify more efficient routes of light olefin production to overcome these disadvantages. Many catalytic processes focusing on "on purpose" light olefin production have been developed to supplement the demand such as propane dehydrogenation, methanol to olefins, olefin metathesis and catalytic cracking of naphtha [2].

✉ Masikana M. Mdleleni
masikana.mdleleni@petrosa.co.za

[1] PetroSA Synthetic Fuels Innovation Center, South African Institute for Advanced Materials Chemistry, University of the Western Cape, Robert Sobukwe Road, Bellville 7535, South Africa

Catalytic cracking of various types of hydrocarbons including naphtha range hydrocarbons has been investigated over ZSM-5 zeolites to produce light olefins. The reaction occurs at much lower temperatures of 550–600 °C compared to steam cracking and the yields of ethylene and propylene are high enough to compete with steam cracking. Additionally, higher P/E ratios is excess of one are attainable compared to 0.4–0.7 for steam cracking [3]. This is highly advantageous as the demand or propylene continues to grow.

Zeolites, in particular ZSM-5 are active catalysts and/or supports for a range of reactions such as cracking, alkylation, aromatization and isomerization of hydrocarbons, due to their activity, shape selectivity [4, 5], ion-exchanging properties, special three dimensional micropore structure and large specific surface area in ZSM-5 [6, 7]. They play a significant part in the olefin industry and in current processes that are under development and modification in order to commercialize these technologies. For instance P/E ratios can be adjusted to meet global demands by controlling the acid type, strength and distribution of Bronsted/Lewis acid sites of the ZSM-5 catalyst as well as the operating conditions of temperature, pressure and WHSV. Other modifications of the ZSM-5 catalyst include alterations of the acidic properties using transition metals [1]. Previous

studies conducted by Lu et al. [8] have shown that Fe and Cr promoted ZSM-5 have good selectivity to C_2 and C_3 olefins in the cracking of Isobutane at 625 °C. This may be due to metals such as Fe and Cr being able to enhance the dehydrogenative cracking of Isobutane. Isobutane when dehydrogenated to isobutene can then be easily cracked to lighter olefins. However, the effect of Fe and Cr metal loading and Cr^{6+}/Cr^{3+} ion ratio on altering the acidity as well as electronic promoter effects to enhance selectivity to olefins is not clearly understood. Therefore, Fe and Cr were seen as a suitable choices as a metal promoters for the cracking of refinery naphtha. Moreover, due to the difference in reactivity of the various compounds present in naphtha, selectivity to valuable olefins may be affected. Further investigations using complex refinery naphthas are required to understand the process under industrial conditions.

In this study we examined the use of Fe and Cr modified ZSM-5 as catalysts for the catalytic cracking of naptha obtained from the Chevron refinery to enhance light olefin selectivity. Catalysts with loadings of 0.5–5 wt% of Fe and Cr have been prepared and its effects of the catalyst properties such as porosity and acidity have been studied. The catalytic performance has also been evaluated and its effect on activity and selectivity to olefins is investigated.

Experimental

Catalyst preparation

Catalysts with different Fe and Cr loadings were prepared using the impregnation method. Fe and Cr (0.5, 2 and 5 wt%) were loaded onto to Zeolyst ZSM-5 ($SiO_2/Al_2O_3 = 30$) using $Fe(NO_3)_3{\cdot}9H_2O$ and $Cr(NO_3)_3{\cdot}9H_2O$ salts. The total mass of impregnated zeolite was 5 g. The appropriate amount of the nitrate salts were dissolved in excess distilled water (25 ml) and stirred until the salt completely dissolved. For example, approximately 0.192 g of $Cr(NO_3)_3{\cdot}9H_2O$ was added to the aqueous solution to obtain a 0.5 wt% metal loading. ZSM-5 was then added to the solution slowly and stirred at 80 °C until all the water had evaporated. It was then left to air dry and was then further dried in an oven at 110 °C overnight. The catalysts were then calcined at 500 °C for 6 h to convert the metals to the oxide form. The metal modified ZSM-5 samples were characterised using XRD, N_2 physisorption, NH_3-TPD, H_2 TPR, HRSEM and EDS.

Characterisation

XRD powder patterns were recorded using a Bruker AXS D8 Advance (Cu-Kα radiation $\lambda K\alpha 1 = 1.5406$ Å) 40 kV in the 2θ range 5°–90°. Surface area measurements and porosity analysis were determined by N_2 adsorption/desorption isotherms at − 196 °C using the Micromeritics Tristar 3000 analyzer. Prior to N_2 physisorption samples were degassed at 150 °C for 4–5 h using helium. NH_3-TPD was used to determine the amount and strength of acid sites in the ZSM-5 zeolites. TPD profiles were obtained using an Autochem II Micromeritics chemisorption analyser. Typically 0.1 g of catalyst is loaded into the reactor. This is then activated by heating rapidly to 500 °C and holding for 20 min under helium flow at 30 ml/min. The catalyst is then cooled to 120 °C under flowing helium. The gas was then switched to 5% NH_3 in balance helium and the NH_3 was adsorbed at 120 °C for 30 min at a flow rate of 15 ml/min. Helium was once again allowed to flow over the catalyst to remove any physisorbed NH_3. Under flowing helium NH_3 desorption occurred. The flow rate was kept constant at 25 ml/min while the temperature was ramped up to 700 °C at a rate of 10 °C/min. The signal was detected using a thermal conductivity detector (TCD) and the outputs recorded on a computer. H_2-TPR was performed to determine the reducibility of the metal impregnated samples as well as to confirm the metal oxide phase. Typically 0.1 g of catalyst is loaded into the reactor. This is then purged with Argon while the cold trap is being prepared. 10% H_2 balance Argon was used in the experiment. The 10% H_2/Ar was allowed to flow over the sample at 50 ml/min as the temperature was ramped to 900 °C at 10 °C/min. Scanning electron microscopy (SEM) micrographs were obtained using a high resolution–SEM EHT 5.00 kV. All samples were carbon coated before imaging. The HRSEM was also equipped with an EDS spectrometer with the AZTEC EDS system by Oxford Instruments for elemental analysis of zeolites.

Catalytic testing

The catalytic performance was evaluated using a stainless steel fixed bed reactor. Typically 0.25 g of catalyst was loaded and supported using quartz beads. The reaction conditions were as follows $T = 550$ °C, $P =$ atmospheric, WHSV = ~ 16 h^{-1}. The feed flow rate was kept at 0.1 ml/min while nitrogen was passed through at 74.8 ml/min to obtain a N_2/Feed ratio of 4:1. Products were analysed by on a Bruker 450-GC. Gas products were analysed on a BR—Alumina–Na_2SO_4 column while liquid products were analysed on a RTX-100-DHA 100 m stationary phase column. The method used to determine product distribution was the ASTM D6729 method. Hydrocarbons in the C_1–C_{14} range were analysed and identified as paraffins, olefins, aromatics and others using PONA analysis. A significant amount of products which could not be identified was grouped as others and was not included in the selectivity to BTEX products. Naphtha conversion was calculated based on the product distribution results obtained from the detailed hydrocarbon analysis (DHA). Naphtha hydrocarbons present in the liquid product were assumed to be unconverted feed

and therefore conversion was calculated as feed hydrocarbons minus product hydrocarbons. This was done for each individual component for example: [C_5=(feed)–C_5=(prod)]. All positive deltas were summed up as they were assumed to be converted hydrocarbons while all negative deltas which represent additional compounds appearing after reaction were considered as zero. The selectivities to C_2–C_5 olefins and BTEX products were calculated only on feed that had been converted. The equations are shown below:

$$\text{Naphtha conversion} = \sum \text{Feed } C_{nA} - \sum \text{Product } C_{nA},$$

where n is the hydrocarbon number and A is the hydrocarbon type, e.g., paraffin.

$$\%\text{Product selectivity} = \frac{\text{Mass component } x_i}{\sum x_i} \times 100$$

Results and discussion

The Fe and Cr loaded ZSM-5 catalysts are characterised using XRD, BET, and NH_3-TPD to determine the structure, porosity and acidity, respectively. The XRD diffractograms of Fe loaded 0.5–5 wt% and Cr loaded 0.5–5 wt% samples are shown in Fig. 1a, b, respectively.

The peaks observed in the patterns in the range 7°–9° and 22°–25° 2θ in both Fig. 1a, b correspond to that of a crystalline ZSM-5 zeolite. From Fig. 1a it is noticed that the ZSM-5 zeolite containing different loadings of Fe in the range 0.5–5 wt% show a slight decrease in intensity of the peaks when compared to the unmodified ZSM-5. The relative crystallinity is calculated and shown in Table 1. Interestingly, the Fe loaded samples show a decrease in crystallinity (90–65%) as the metal loading increases from 0.5 to 5 wt% indicating that the impregnation with Fe may cause

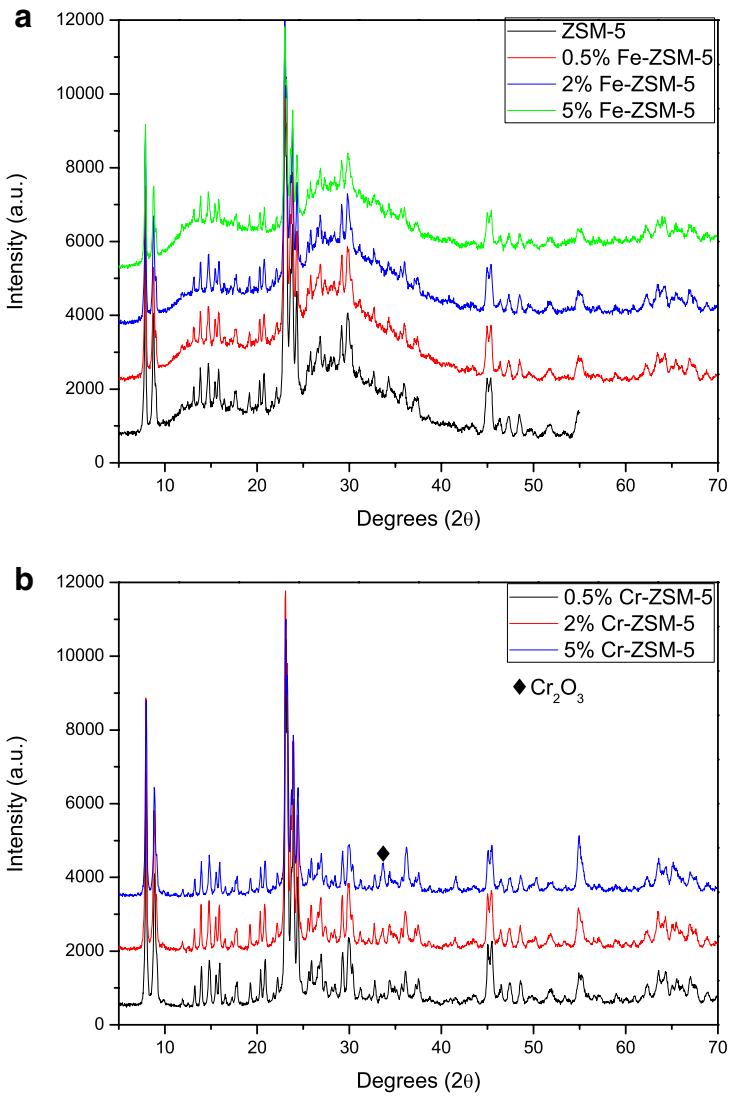

Fig. 1 **a** XRD diffractograms of ZSM-5 with different Fe metal loadings (0.5–5 wt%). **b** XRD diffractograms of ZSM-5 with different Cr metal loadings (0.5–5 wt%) and diamond marking peak corresponding to Cr_2O_3 phase

Table 1 BET and NH_3-TPD results of Fe and Cr modified ZSM-5 catalysts

Sample	Rel. cryst[a] (%)	SSA (m^2/g)	Micropore s/a (m^2/g)[b]	External[a] s/a (m^2/g)	Pore vol. (cm^3/g)[c]	Acid sites[d]			
						Peak 1		Peak 2	
						Acidity (μmol/g)	T_{max} (° C)	Acidity (μmol/g)	T_{max} (° C)
ZSM-5	100	350	223	127	0.21	443	193	190	395
0.5% Fe	90	341	207	134	0.22	407	183	75	375
2% Fe	87	332	210	122	0.21	336	180	55	387
5% Fe	65	317	203	114	0.20	359	187	59	391
0.5% Cr	100	331	208	123	0.21	443	200	130	395
2% Cr	100	320	209	111	0.22	395	195	123	378
5% Cr	90	308	195	113	0.20	363	194	79	382

[a]Relative crystallinity determined from the five most intense XRD peaks in the 7°–9° and 22°–25° 2θ range

[b]Areas determined using *t* plot

[c]Determined using BJH method

[d]Acidity determined by NH_3-TPD measurements

some change to the structure of the ZSM-5. Similar effects were observed by de Oliveira et al. [9] on iron impregnated ZSM-5 in the 2.5–5 wt% range. Furthermore, no peaks corresponding to that of iron oxide could be detected. This may be due to the metal loading being too low or the iron crystallites too small for X-ray diffraction indicating a high dispersion [10].

In Fig. 1b it is also noticed that the modification of ZSM-5 zeolite with Cr (0.5–5 wt%) by impregnation method did not affect the crystallinity of ZSM-5 as observed with the Fe modified catalysts. Chromium oxide can exist in two phases, i.e., CrO_3 and Cr_2O_3 corresponding to Cr(VI) and Cr(III), respectively. It is possible that both phases may be present in the sample; however, peaks corresponding to the CrO_3 phase are overlapped by ZSM-5 peaks. As the loading increases from 0.5 to 5% it is noticed that there is slight increase in intensity of the peak at 33.6° 2θ. This peak corresponds to chromium oxide(Cr_2O_3) confirming the presence of chromium on the 5 wt% Cr loaded sample [11].

The physicochemical properties, acidity and porosity of Fe and Cr impregnated ZSM-5 were performed using NH_3-TPD and N_2 physisorption, respectively. The results are shown in Table 1 below.

The un-modified ZSM-5 has both the largest micropore and external surface areas summing up to the highest SSA of 350 m^2/g. After metal loading the SSA is seen to decrease and decreases further with increasing Fe and Cr loading from 0.5 to 5 wt%. A smaller decrease in the external surface area compared to micropore surface area is observed with increased metal loading from 0.5 to 5 wt% for both Fe and Cr modified samples. For both metals, samples with the highest loadings have the lowest micropore surface areas. This suggests that Fe and Cr metals are located in the micropores of the zeolite which leads to pore blocking. The surface areas for Cr-modified ZSM-5 compared to Fe are slightly lower for all comparable loadings. This may be due to a difference in metal particle size and dispersion.

The un-modified ZSM-5 also has the highest amount of acidity. The total acidity decreases with an increase in metal loading from 0.5 to 5 wt% for both Fe and Cr modified samples. As shown in Fig. 2a, b, two peaks are observed in the NH_3-TPD profiles at approximately 190 and 390° C corresponding to weak and strong acid sites, respectively. As noticed in the TPD profiles, the area of the second peak corresponding to stronger acid sites which may include Bronsted sites originating from framework aluminium within the micropores decreases with increasing metal loading. It is possible that by metal particles blocking the micropores of the zeolite access to stronger acid sites are restricted. Although the effect of Fe and Cr loading on the ZSM-5 surface area was quite similar, interestingly Fe has a greater effect on the acidity in particular the amount of strong acid sites. As noticed in Table 1, Fe loading causes a much larger decrease in the amount of strong acid sites than Cr for all analogous weight loadings. This may be due to a difference in metal particle size and dispersion as well as metal/acid site interaction. Lai et al. [10] have shown using UV–Vis spectroscopy that Fe can exist as isolated Fe^{3+} species, Fe_xO_y oligomeric clusters and Fe_xO_y nanoparticles which can easily access the pore network of ZSM-5. Krishna and Makkee [12] have also reported Fe species associated with framework alumina using NO DRIFTS. From the XRD Fe could not be detected whereas Cr at higher loading was present indicating that Cr may have a larger particle size and less dispersion and therefore less interaction with strong Bronsted acid sites than Fe.

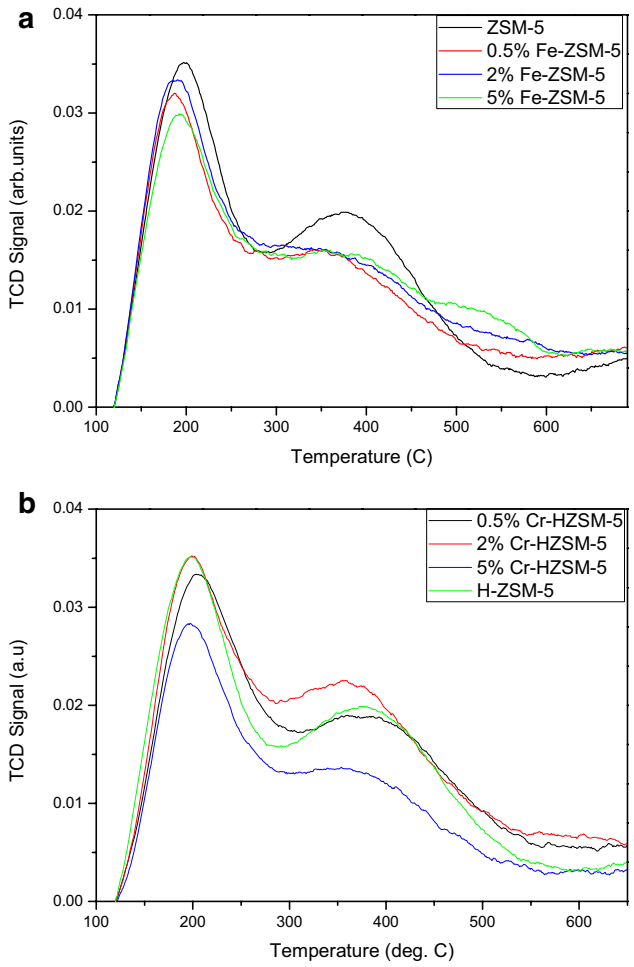

Fig. 2 **a** NH_3-TPD profiles of unmodified and Fe loaded ZSM-5 catalysts. **b** NH_3-TPD profiles of unmodified and Cr loaded ZSM-5 catalysts

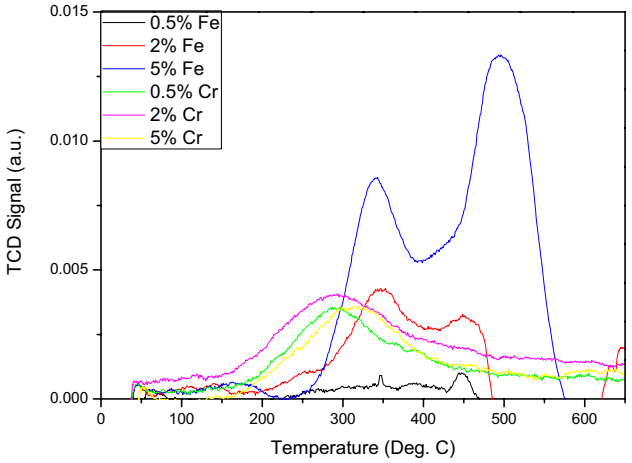

Fig. 3 H_2-TPR profiles of Fe an Cr modified ZSM-5 with weight loadings (0.5, 2 and 5 wt%)

H_2-TPR was used to confirm the reducibility characteristics and metal species present in the samples. The profiles of Fe and Cr- modified ZSM-5 are shown in Fig. 3 and the peak concentrations are shown in Table 2.

From the profiles in Fig. 3 it can be observed that there are two reduction maxima for the Fe modified ZSM-5 at approximately 350 °C and 450–500 °C. This corresponds to the reduction of Fe_2O_3 to Fe_3O_4 ($Fe^{3+} \rightarrow Fe^{2+}$) and Fe_3O_4 to Fe metal ($Fe^{2+} \rightarrow Fe^0$), respectively [13]. It is also noticed that the area under the reduction peaks increase as the iron loading increases as more hydrogen is being consumed in the reduction reaction. The H_2 uptake is shown in Table 2 and increases from 12 µmol/g for the 0.5% Fe to 337 µmol/g for 5% Fe. The reduction temperature also increases from approximately 450 to 500 °C.

The Cr doped ZSM-5 samples exhibit a single reduction peak. A broad peak from 200 to 450 °C with a maximum at approximately 300 °C can be attributed to the reduction of $Cr^{6+} \rightarrow Cr^{3+}$ species corresponding to the reduction of CrO_6 to Cr_2O_3. It is known that loadings of 5 wt% and less generally exist in the Cr^{6+} form [14–16] and as loadings increase chromium may exist as α-Cr_2O_3. Michorczyk et al. [15] have shown that Cr content above 3.4 wt% results in the appearance of an additional low temperature reduction peak at approximately 280 °C, which coincides with the reduction of crystalline α-Cr_2O_3 rom a Cr^{6+} to a Cr^{3+} [17] or Cr^{2+} [11] species. Thus, it is possible that the Cr modified samples contain both CrO_3 and Cr_2O_3 phases as the broad peaks observed in the TPR profiles extend over the temperature ranges in which both phases are reduced. Furthermore, the Cr_2O_3 phase was detected by XRD for the 5% Cr sample further supporting this notion. It may be worthwhile to conduct an XPS analysis to confirm the Cr^{6+}/Cr^{3+} ratio as the two species have a different effect on the catalytic performance.

SEM, EDS and XRF analysis were used to confirm the ZSM-5 Si/Al ratio and metal loading. The results are shown in Table 3.

From Table 3 it is noticed that the average Si/Al molar and atomic ratios as determined by XRF and EDS are about 30 and 17, respectively, for all samples and are close to the given Si/Al ratio of the commercial Zeolyst ZSM-5. Thus,

Table 2 Hydrogen consumption for the Fe and Cr loaded ZSM-5 samples

Sample	H_2 consumption (µmol/g)	
	Peak 1	Peak 2
0.5% Fe	1	11
2% Fe	44	45
5% Fe	104	233
0.5% Cr	135	
2% Cr	152	
5% Cr	169	

Table 3 XRF and EDS analysis of Fe and Cr modified ZSM-5

Sample	Si/Al ratio-XRF[a]	Si/Al ratio-EDS[b]	Metal loading (%)			
			XRF		EDS	
			Fe	Cr	Fe	Cr
ZSM-5	31.6	15	–	–	–	–
0.5% Fe	33	17.2	0.8		–	
2% Fe	31.5	17.0	2.6		2.0	
5% Fe	31.1	17.1	6.4		3.9	
0.5% Cr	30.8	16.6		0.3		1.3
2% Cr	30.4	15.9		0.9		3.1
5% Cr	30.4	18.2		2.1		11.0

[a]Molar ratio from XRF analysis

[b]Atomic ratio from EDS analysis

metal loading by impregnation method has not resulted in dealumination of the zeolite. The metal loadings as determined by XRF show that ZSM-5 impregnated with Fe are in close agreement with the theoretical loadings and all sample was successfully loaded onto the zeolite. However, the ZSM-5 loaded with Cr seems to be slightly below the theoretical loadings of 0.5, 2 and 5 wt% for all analogous loadings. The metal loading for the 0.5% Fe sample could not be detected by EDS analysis. This may be due to the loading being below the detection limit of 1 wt%. However, for the 2% Fe and 5% Fe samples the metal detected by EDS increases as the loading increases and is in agreement with the batch loading. Interestingly, the Cr metal loading percentages determined by EDS are slightly higher with the 5% Cr sample having a loading of ~ 11%. Although lower loadings were detected by XRF the higher loadings observed with EDS analysis may be due to lower dispersion and clustering of Chromium particles on the zeolite compared to that of Iron. X-ray mapping of the samples with the highest loadings, i.e., 5% Fe and Cr was conducted and is shown in Fig. 4. The results show that both Fe and Cr are well dispersed although chromium appears to have a greater amount of metal present on the surface and small clusters are visible.

Catalytic performance

ZSM-5 was modified with Fe and Cr via the incipient wetness impregnation method. ZSM-5 was loaded with 0.5, 2 and 5 wt% Fe. The catalysts were calcined at 500 °C for 6 h to convert Fe and Cr to the oxide form. The catalysts were then used in the cracking of Naphtha at the following reaction conditions, i.e., $T = 550$ °C, WHSV = 16 h^{-1}, N_2: Naphtha feed ratio of 4:1 at atmospheric pressure. Naphtha obtained from Chevron was analysed prior to being used as a feed to determine the hydrocarbon composition. This was done by GC analysis and the Detailed Hydrocarbon Analysis (DHA) software. The composition is shown in Table 4.

The results of the catalyst activity and selectivity are shown below. The effect of metal loading on the activity of the catalysts is shown in Fig. 5 and is compared to the parent ZSM-5.

Figure 5 shows the conversions as a function of time on stream for the various metal modified catalysts. It is noticed that the initial conversions are in the range of 44–56%. The parent ZSM-5 catalyst has the highest initial conversion of 56%. The initial conversions are lower for metal modified catalysts compared to the parent ZSM-5. As the Fe loading increases from 0.5 to 5% the initial conversion decreases from ~ 55 to 47%. This may be due to Fe particles blocking stronger Bronsted sites responsible for cracking reactions. The Cr modified ZSM-5 catalysts have initial conversions much lower than the Fe modified catalysts. The 2% Cr–ZSM-5 has the lowest conversion of 44%. No clear trend is observable as to the effect of chromium loading on the conversion of naphtha as the 5% Cr has a slightly higher initial conversion than the 2% Cr and is similar to 0.5% Cr catalyst. As the reaction proceeds, all catalysts show some deactivation. Interestingly, The Fe promoted catalysts show a lesser decrease in activity between the initial and final conversions. The parent ZSM-5 shows the largest decrease of approximately 12%. As the Fe loading increases the reduction in activity is less significant with the 5% Fe–ZSM-5 only decreasing by 5%. Thus, it can be said that modification with Fe enhances the stability of the catalyst. The Cr catalysts also show some slight deactivation. The 0.5 and 5% Cr catalysts show similar stability. However, the 2% Cr catalyst which had the lowest initial conversion seems to be the most stable of the Cr modified catalysts.

The effect of Fe and Cr on the selectivity to lower olefins, i.e., C_2–C_5 olefins for the third and last hours of the reaction is shown in Table 5.

All the Fe modified catalysts show a similar selectivity to total olefins in the third hour of the reaction of ~ 48% with a slight decrease observed for the 5% Fe catalyst. The same

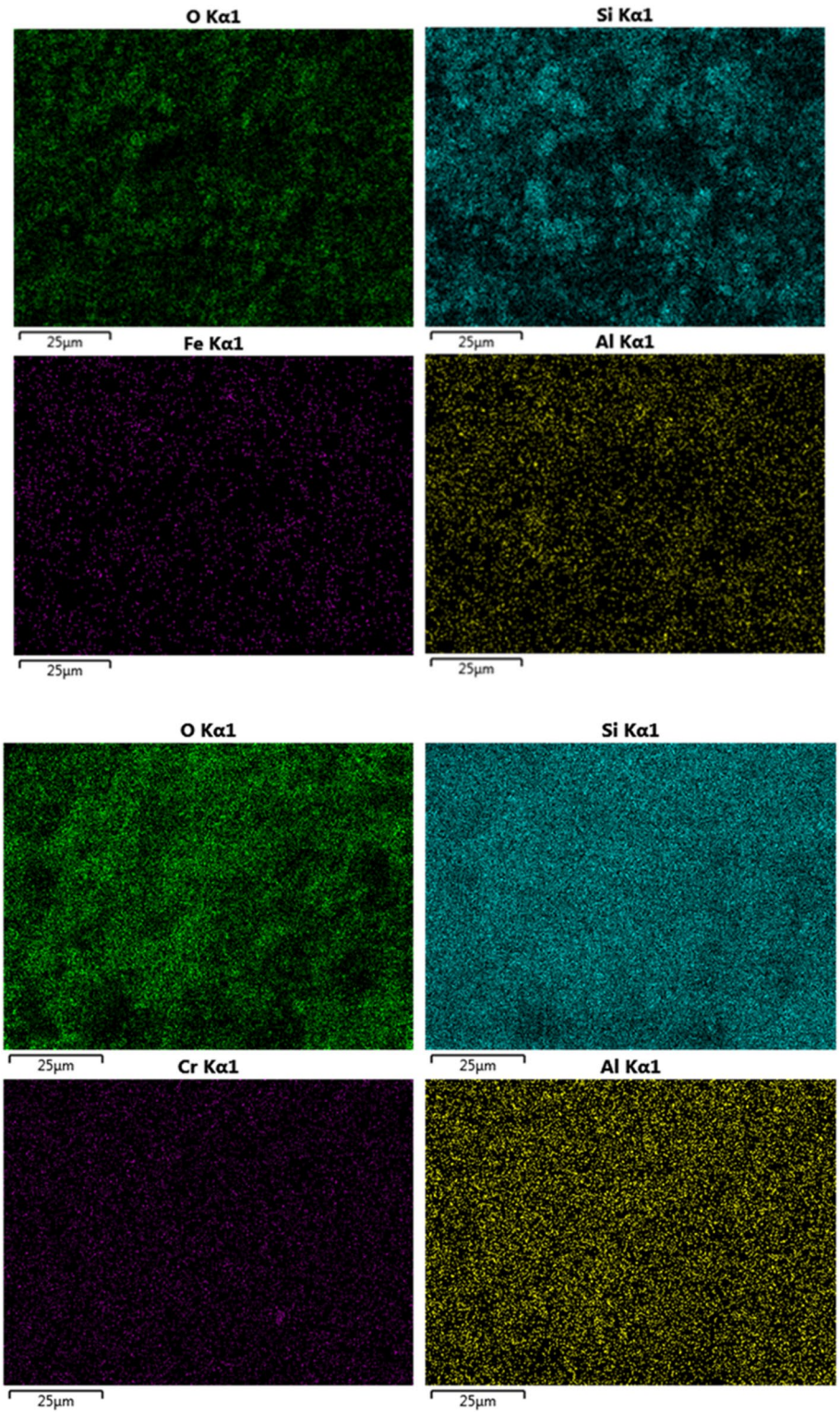

Fig. 4 X-ray mapping of 5% Fe and 5% Cr ZSM-5 samples

trend is observed for the selectivity to propylene of which the 5% Fe has the lowest (16.2%). The 2% Fe catalyst has the highest selectivity to propylene of 21.6%. The trend indicates that the selectivity to total olefins and propylene is related to the conversion. As the conversion in the third hour decreases the selectivity also decreases. However, in the last hour of the reaction in which the conversion is lower than in the third hour for all catalysts the selectivity to total olefins increases. This is due to the increase in C_5 olefins. The selectivity to propylene tends to decrease except

Table 4 Hydrocarbon composition of naphtha obtained from Chevron

	Paraffins Cyclo	Paraffins Iso	Paraffins Normal	Olefins Cyclo	Olefins Iso	Olefins Normal	Aromatics	Others	Total
Naphtha feed									
C_3	0	0	0.03	0	0	0.06	0	0	0.09
C_4	0.47	0.77	0	0	4.5	1.27	0	0.56	7.57
C_5	0.39	1.73	0.85	0.67	15.15	0	0	0.66	19.45
C_6	0.1	2.05	0	0.77	7.93	0	2.42	4.166	17.436
C_7	0.86	1.42	0.52	0.05	7.91	1	3.31	0.585	15.655
C_8	2.17	1.3	0	0	4.29	0.05	5.91	0.275	13.995
C_9	1.36	2.6	0.29	0	1.35	0.25	5.01	0	10.86
C_{10}	0.07	3.54	0.35	0	0.2	0	3.65	0.075	7.885
C_{11}	0	2.75	0.23	0	0	0	2.58	0.686	6.246
C_{12}	0	0	0.12	0	0	0	0.32	0.373	0.813
Total	5.42	16.16	2.39	1.49	41.33	2.63	23.2	7.38	100

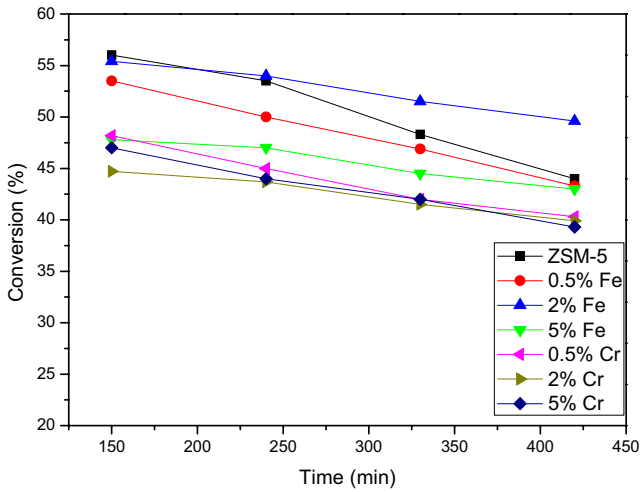

Fig. 5 Naphtha conversions as a function of time over the parent and metal modified ZSM-5 catalysts

for the 2% Fe–ZSM-5 catalyst in which a slight increase is observed. The trend that selectivity is related to conversion is maintained as the 2% Fe–ZSM-5 catalyst has the highest conversion in the last hour approximately 50% and the highest selectivity to total olefins of 60% is obtained. The results indicate that a conversion of 50% and above needs to be maintained for high propylene selectivity and the optimum metal loading seems to be 2%. The Fe promoted catalysts also show a lesser decrease in selectivity to propylene with time compared to the parent ZSM-5 with the highest metal loading of 5% Fe–ZSM-5 catalyst having the smallest decrease. This is related to the enhanced stability of 5% Fe–ZSM-5 catalyst. Therefore, the results indicate that modification with Fe enhances both selectivity to olefins and the stability of the catalyst.

The selectivities to C_2 and C_3 for the Cr modified catalysts decrease slightly from the third to the last hour and follow the trend that at higher conversions higher selectivities

Table 5 Selectivity to olefins in the gas product for parent, Fe and Cr modified ZSM-5

Olefin selectivity	ZSM-5		0.5% Fe		2% Fe		5% Fe	
	Third hour	Last hour	Third hour	Last hour	Third hour	Last hour	Third hour	Last hour
C_2	9.0	2.0	6.3	3.6	8.3	5.4	4	2.6
C_3	20.8	12.6	19.0	14.9	21.6	23.6	16.2	13.5
C_4	7.6	11.7	8.7	8.4	8.7	10.9	8.7	11.2
C_5	10.7	26.2	14.6	24.2	8.7	21.4	16.4	23.6
Total	48.1	52.5	48.6	51.1	47.3	61.3	45.3	50.9
Olefin selectivity	0.5% Cr		2% Cr		5% Cr			
	Third hour	Last hour	Third hour	Last hour	Third hour	Last hour		
C_2	3.0	1.9	3.1	1.7	3.4	1.5		
C_3	9.7	8.1	9.0	5.7	11.4	7.0		
C_4	11.1	11.3	9.9	7.2	9.9	10.3		
C_5	12.7	16.2	19.0	16.6	13.3	25.0		
Total	36.5	37.5	41.0	31.2	38.0	43.8		

are observed. Interestingly, no change in selectivity to ethylene or propylene is observed for an increase in chromium loading. The ethylene and propylene selectivity in the third and last hours of the reaction of 3 and 1.7% and approximately 10 and 7%, respectively, is maintained. Selectivity to C_4 olefins remains constant for all catalysts while a slight increase to C_5 olefins is noticed. However, when compared to Fe modified catalysts the Cr catalysts have a much lower selectivity to lower olefins (C_2–C_5) in both the third and last hours of the reaction. A difference of 30% is observed when 2% Fe is compared to 2% Cr in the last hour. This indicates that Fe is a better promoter to enhance selectivity to light olefins than Cr. It is possible that the difference in acidity is responsible for the difference in selectivity. As the Cr ZSM-5 has slightly higher total acidities when compared to Fe, readsorption of light olefins on acid sites may occur leading to secondary aromatisation reactions thus also indicating zeolites with a lower acid site density would give selectivity to light olefins while suppressing aromatics formation [18].

The selectivity to liquid products for the metal modified catalysts is shown in Fig. 6. The hydrocarbon composition of the liquids range from C_5 to C_{14} and consist of aromatics, paraffins, naphthenes and olefins as observed from GC analysis using a DHA column of which aromatics make up the bulk of the product. From the graph it is noticed that the selectivity to liquids remains constant for the parent ZSM-5 in the initial and final hour of the reaction. Interestingly, the Fe and Cr modified ZSM-5 show stark differences in selectivity. The Cr–ZSM-5 catalysts show higher selectivities compared to Fe–ZSM-5 catalysts in the initial hours of the reaction. As the reaction proceeds, the Cr catalysts increase in selectivity, whereas the Fe catalysts decrease. Remarkably the 2% Cr catalyst has the highest increase in selectivity to liquid products (~65%) compared to the 2% Fe which shows the largest decrease in selectivity (~35%). From the results of selectivity to gas olefins the 2% Fe had the greatest selectivity therefore it is expected that it would have a lower selectivity to olefins. However, this may suggest that Cr catalysts actually promote aromatics production of which the 2% Cr–ZSM-5 is the best catalyst.

A plot of the selectivity to BTEX products is shown in Fig. 7.

From Fig. 7 it is noticed that BTEX selectivity is higher initially for all Fe catalysts (~20–24%) and decreases with time on stream as the conversion decreases to between 13 and 15%. No clear trend is observed with respect to BTEX selectivity However, it is evident that the Cr–ZSM-5 catalysts are more selective to aromatic products than Fe–ZSM-5 and reaches a maximum for the 2% Cr-catalyst. The 2% Cr catalyst has the highest selectivity of ~29% of which the composition is mainly toluene and xylenes and small amount

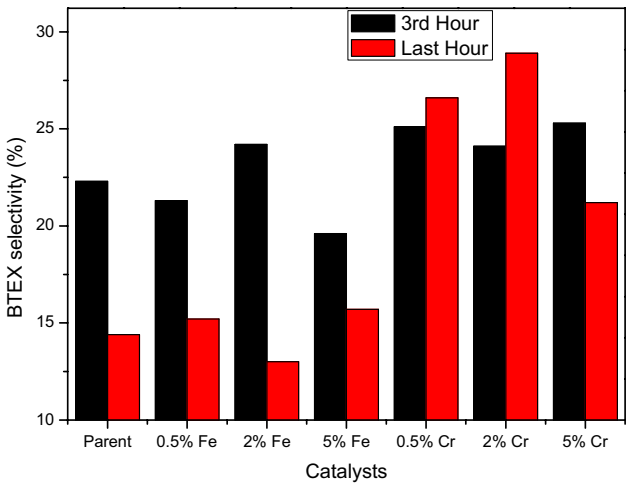

Fig. 7 Bar graph showing selectivity to BTEX products for all metal modified catalyst

Fig. 6 Total liquid product selectivity of metal modified catalysts

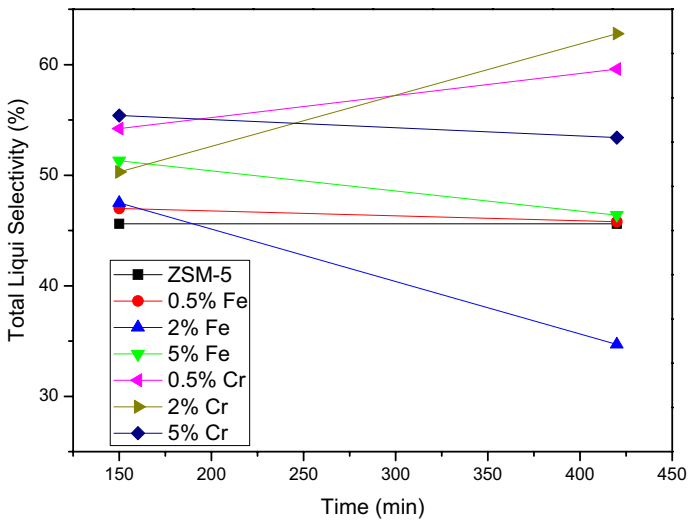

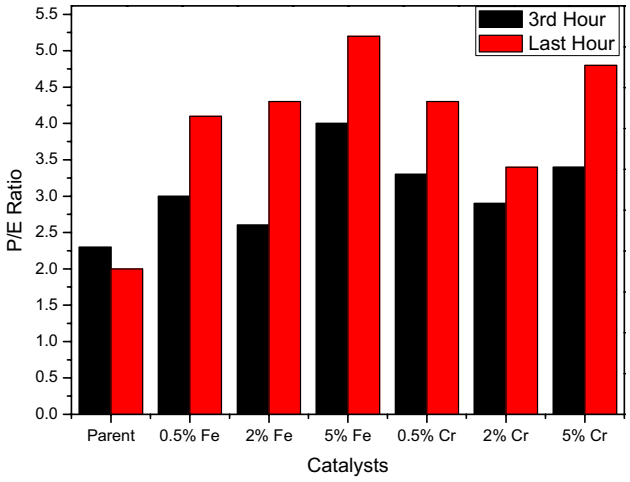

Fig. 8 P/E ratios for all metal-modified catalysts

of benzene is produced. Lu et al. [8] have shown that Cr in small amounts between 0.004 and 0.038 mmol/g alters acidity and plays an important role in promoting cracking of isobutane and dehydrogenation of isobutane to isobutene which is then easily cracked to lighter olefins and is similar to iron in promotional effects. However, the differences in product distribution observed in this study between Fe and Cr modified samples indicate different promotional mechanisms in the cracking of refinery naphtha. In particular Cr ions are shown to favour aromatization and alkylation reactions. The chromium loadings in our study fall in the range of 0.059–0.409 mmol/g which is higher than the range established by Lu et al. [8] for promotion of dehydrogenative cracking which may suggest that higher loadings of chromium above 0.038 mmol/g may promote aromatization reactions. The exact cause, i.e., role of acidity and metal support interaction is not clearly understood and further analysis of the amount of Lewis and Bronsted acid sites as well as XPS and DRIFTS analysis may be required to elucidate the role of the Fe and Cr ions.

The propylene to ethylene P/E ratios were calculated for all catalysts and are shown in Fig. 8.

It is clearly observed that Fe enhances the P/E ratio as all Fe-modified catalysts have a better ratio than the parent ZSM-5. The P/E ratio is also observed to increase with an increase in Fe loading with the 5% Fe–ZSM-5 having the highest P/E ratio of five. Thus, the addition of Fe enhances selectivity to propylene and has a decreased selectivity to ethylene. The P/E ratios for Cr catalysts seem to show that it goes through a minimum for the 2% Cr catalyst after which it increases. This makes sense since the 2% catalyst was the best promoter of BTX products. The increase observed with an increase to 5% Cr loading may be related to the ratio of Cr^{6+}/Cr^{3+} ions but further analysis is required to verify.

Conclusion

Metal modification with Fe and Cr had an effect on both the physicochemical properties of the catalysts as well as the catalytic performance. Metal loading did not affect the crystallinity of the ZSM-5 but caused a decrease in the specific surface area which decreased further with increased metal loading. Fe had a greater effect on the total acidity in particular strong acid sites when compared to Cr. Fe acted as a promoter of both selectivity to olefins, in particular propylene as well as enhanced the stability of the catalyst. The best results were achieved with a Fe loading of 2% which gave the greatest selectivity to propylene of 23.6% and total olefin selectivity of 60%. Furthermore Fe modification improved the P/E ratio from two to a maximum of five. Cr modification was found cause a decrease in selectivity to lower olefins and an increase in selectivity to BTX products. The highest selectivity to BTX of ~ 65% was obtained with the 2% Cr–ZSM-5 catalyst.

Acknowledgements The authors would like to thank the Petroleum, Oil and Gas Corporation of South Africa (PetroSA) for their financial support and technical discussions, the electron microscope unit, Physics Department, University of the Western Cape for the SEM images and Ithemba labs for the XRD work.

References

1. Rahimi N, Karimzadeh R (2011) Catalytic cracking of hydrocarbons over modified ZSM-5 zeolites to produce light olefins: a review. Appl Catal A Gen 398:1–17. https://doi.org/10.1016/j.apcata.2011.03.009
2. Mitchell S, Boltz M, Liu J, Pérez-Ramírez J (2017) Engineering of ZSM-5 zeolite crystals for enhanced lifetime in the production of light olefins *via* 2-methyl-2-butene cracking. Catal Sci Technol 7:64–74. https://doi.org/10.1039/C6CY01009A
3. Sattler JJHB, Ruiz-Martinez J, Santillan-Jimenez E, Weckhuysen BM (2014) Catalytic dehydrogenation of light alkanes on metals and metal oxides. Chem Rev 114:10613–10653. https://doi.org/10.1021/cr5002436
4. Bellussi G, Pollesel P (2005) Industrial applications of zeolite catalysis: production and uses of light olefins. Stud Surf Sci Catal 158:1201–1212. https://doi.org/10.1016/S0167-2991(05)80466-5
5. Degnan TF (2003) The implications of the fundamentals of shape selectivity for the development of catalysts for the petroleum and petrochemical industries. J Catal 216:32–46. https://doi.org/10.1016/S0021-9517(02)00105-7

6. Jung JS, Park JW, Seo G (2005) Catalytic cracking of *n*-octane over alkali-treated MFI zeolites. Appl Catal A Gen 288:149–157. https://doi.org/10.1016/j.apcata.2005.04.047
7. Corma A (1993) Transformation of hydrocarbons on zeolite catalysts. Catal Lett 22:33–52. https://doi.org/10.1007/BF00811768
8. Lu J, Zhao Z, Xu C et al (2006) CrHZSM-5 zeolites—highly efficient catalysts for catalytic cracking of isobutane to produce light olefins. Catal Lett 109:65–70. https://doi.org/10.1007/s10562-006-0058-2
9. De Oliveira TKR, Rosset M, Perez-Lopez OW (2018) Ethanol dehydration to diethyl ether over Cu-Fe/ZSM-5 catalysts. Catal Commun 104:32–36. https://doi.org/10.1016/j.catcom.2017.10.013
10. Lai S, She Y, Zhan W et al (2016) Performance of Fe–ZSM-5 for selective catalytic reduction of NO_x with NH_3: effect of the atmosphere during the preparation of catalysts. J Mol Catal A Chem 424:232–240. https://doi.org/10.1016/j.molcata.2016.08.026
11. Hakuli A, Harlin ME, Backman LB, Krause AOI (1999) Dehydrogenation of *i*-Butane on CrO_x/SiO_2 Catalysts. J Catal 184:349–356
12. Krishna K, Makkee M (2006) Preparation of Fe–ZSM-5 with enhanced activity and stability for SCR of NO_x. Catal Today 114:23–30. https://doi.org/10.1016/j.cattod.2006.02.002
13. Long RQ, Yang RT (2000) Characterization of Fe–ZSM-5 catalyst for selective catalytic reduction of nitric oxide by ammonia. J Catal 194:80–90. https://doi.org/10.1006/jcat.2000.2935
14. Cheng Y, Miao C, Hua W et al (2017) Cr/ZSM-5 for ethane dehydrogenation: enhanced catalytic activity through surface silanol. Appl Catal A Gen 532:111–119. https://doi.org/10.1016/j.apcata.2016.12.025
15. Michorczyk P, Ogonowski J, Kuśtrowski P, Chmielarz L (2008) Chromium oxide supported on MCM-41 as a highly active and selective catalyst for dehydrogenation of propane with CO_2. Appl Catal A Gen 349:62–69. https://doi.org/10.1016/j.apcata.2008.07.008
16. Sohn JR, Ryu SG (2001) Redox and catalytic behaviors of chromium oxide supported on zirconia. Catal Lett 74:105–110. https://doi.org/10.1023/A:1016643232442
17. Grzybowska B, Słoczyński J, Grabowski R et al (1998) Chromium oxide/alumina catalysts in oxidative dehydrogenation of isobutane. J Catal 178:687–700. https://doi.org/10.1006/jcat.1998.2203
18. Hodoshima S, Motomiya A, Wakamatsu S et al (2016) Catalytic conversion of light hydrocarbons to propylene over MFI-zeolite/metal-oxide composites. Microporous Mesoporous Mater 233:125–132. https://doi.org/10.1016/j.micromeso.2015.12.044